International Journal of Thin Film Science and Technology

Volume 9
Issue 3 *Sep. 2020*

Article 1

2020

Design and Fabrication of Broadband Dielectric Mirrors in the Visible Range

Ali Jebelli
Department of Electronics, Carleton University, Ottawa, Canada, ali.jebelli@carleton.ca

Hicham Chaoui
Department of Electronics, Carleton University, Ottawa, Canada, ali.jebelli@carleton.ca

Hossein Kazemi
Department of Electrical Engineering, Quchan University of Technology, Quchan, Iran, ali.jebelli@carleton.ca

Arezoo Mahabadi
Department of Basic Engineering Science, Tehran University, Tehran, Iran, ali.jebelli@carleton.ca

Balbir Dhillon
Mechanical Engineering, University of Ottawa, Ottawa, Canada, ali.jebelli@carleton.ca

International Journal of Thin Films Science and Technology

http://dx.doi.org/10.18576/ijtfst/090301

Design and Fabrication of Broadband Dielectric Mirrors in the Visible Range

Ali Jebelli [1,*] *Hicham Chaoui* [1] *, Hossein Kazemi*[2] *, Arezoo Mahabadi*[3] *and Balbir Dhillon* [4]

[1] Department of Electronics, Carleton University, Ottawa, Canada
[2] Department of Electrical Engineering, Quchan University of Technology, Quchan, Iran
[3] Department of Basic Engineering Science, Tehran University, Tehran, Iran
[4] Mechanical Engineering, University of Ottawa, Ottawa, Canada

Received: 21 Feb. 2020, Revised: 22 Mar. 2020, Accepted: 24 Mar. 2020.
Published online: 1 Sep. 2020.

Abstract: A broadband dielectric mirror in the visible spectrum is made by putting together two quarter-wavelength stacks with two different reference wavelengths, and for smoothing the mirror's spectrum, the gradient algorithm has been used. This mirror consists of 39 layers that have been fabricated by alternative deposition of zinc sulfide and Cryolite, using vacuum thermal evaporation on a glass substrate. The Mirror's reflectance spectrum was measured and it was found close to ideal state.

Keywords: Dielectric mirrors, gradient algorithm, quarter-wavelength stack.

1. Introduction

Using metal mirrors has been very common in the past. Such mirrors, rather than their simple manufacturing process, are also very inexpensive [1]. However, its scope of application is restricted due to the high absorption coefficient of metals. In order to construct high power systems such as laser generators used in optical telecommunication or Interferometers with thin strips, dielectric mirrors should be used [2-6]. For a mirror fabricated with ZnS and cryolite, it is easy to reach the absorption level of less than 0.5%. Yet, in a desirable situation, an absorption level near 0.001% has been reported. In this study, we briefly discuss dielectric mirrors first. Then the design, fabrication of broadband mirrors as well as the results of measuring their reflectance spectra have been presented, accompanied by a conclusion at the end.

2. Dielectric Mirrors

In dielectric mirrors, with an alternative deposition of layers with high (n_L) and low (n_H) refraction coefficients and with the thickness of a quarter-wavelength, we can obtain the maximum reflection.

That's because when the light beams reflects from the layer's interface reaching the mirror's front, they'll accumulate on top of each other in the same phase and will be combined constructively. These mirrors, despite their advantages, are confronted with two problems: i) phase displacement of the reflected beam and ii) limited reflection bandwidth.

If the layers are arranged in a way that the outer layers would be made of a material with a high refraction coefficient, the phase displacement becomes zero. Thus, the optical admittance becomes:

$$Y = \left(\frac{n_H}{n_L}\right)^{2p} \frac{n_H^2}{n_S} \quad (1)$$

Where n_S is the substrate's refraction coefficient, and (2p+1) shows the number of layers. Reflection of the environment is [7]:

$$R = \left(\frac{1-Y}{1+Y}\right)^2 \quad (2)$$

Although the aforementioned equations indicate that as the layer number increases, the admittance and therefore, the reflection increases; but for the bandwidth of the reflection area, the changes do not follow the indicated pattern. According to the following equation, the approximate bandwidth of the reflection area is not related to the number of layers [3,8].

$$\frac{\Delta\lambda}{\lambda_0} = \frac{4}{\pi}\sin^{-1}\left(\frac{n_H - n_L}{n_H + n_L}\right) \quad (3)$$

Where λ_0 is the reference wavelength, and $\Delta\lambda$ is the bandwidth of the reflection band.

*Corresponding author E-mail: ali.jebelli@carleton.ca

3. Designs

If we use equation 3 for a mirror fabricated with n_H= 2.3 for ZnS and n_L = 1.35 for cryolite, the bandwidth of the reflection area becomes:

$$\Delta\lambda = 0.335\lambda_0 \quad (4)$$

This equation indicates that as the wavelength increases, as it advances to the infrared zone, the bandwidth of the reflection area expands. In the visible range (400 to 700 nm) with the reference wavelength of 550 nm, the bandwidth would be 184 nm.

It is evident that if a mirror is needed for the entire visible range (300 nm), a mirror with the bandwidth of 184 nm would not be enough.

Pension and Stemwedel offered a solution, by harmonically increasing the thickness of layers (1955). Then, Heavens & Liddell presented a similar solution, using arithmetic or geometrical increase of the layers [5]. After the construction of computers, various algorithms have been presented and Liddell has evaluated them [6]. Using the gradient algorithm for this purpose has not been reported until now.

The method used here is based on putting together two band-limited mirrors. One of these mirrors reflects the lower reflection region and the other one, the upper region. Reference wavelengths are respectively 455 nm for the first and 605 nm for the second mirror. Since the construction issues don't let us increase the number of layers, we have settled to the minimum number of band-limited mirrors, even though it is definitely better if we use more mirrors.

In order that both of the band-limited mirrors have the ability of 100% reflection, their number of layers must be at least 17. Thus, we chose two mirrors, each with 19 layers with the arrangement of $[H\ L]^9$ H. a quarter-wavelength layer L is also added in order to avoid the transmission hole connecting the two quarter-wavelength layers H. By employing equation 2, 100% reflection in the reference wavelength is guaranteed for both mirrors.

4. Gradient Descent Algorithm

Since combining two band-limited mirrors on the edges and at the center of the reflection area of the final filter creates holes, the gradient algorithm is used to solve this issue and smooth the area. In this algorithm, the thickness of the layers is adjusted so that the minimum root means square error of the desired spectrum, and the mirror spectrum is minimized. In this algorithm, the adjustment of thicknesses is done based on the following equations [5,6,9,10]:

$$\vec{d}^{(i+1)} = \vec{d}^{(i)} - s.\vec{\nabla}MF \quad (5)$$

Where $\vec{d}^{(i)}$and $\vec{d}^{(i+1)}$ are vectors showing the thickness of layers at stage *i* and *i+1* and s is the step length. The gradient vector $\vec{\nabla}MF$ equals:

$$\vec{\nabla}\mathrm{MF} = \left\{\frac{\partial \mathrm{MF}}{\partial \mathrm{d}_1}, \frac{\partial \mathrm{MF}}{\partial \mathrm{d}_2}, \ldots, \frac{\partial \mathrm{MF}}{\partial \mathrm{d}_L}\right\} \quad (6)$$

And the merit function MF is [11]:

$$\mathrm{MF} = \sqrt{\frac{1}{m}\left[\sum_{j=1}^{m}\left(R_j^C - R_j^D\right)^2\right]} \quad (7)$$

Where R_j^D and R_j^C are the desired spectrum and the calculated spectrum at point j, respectively. The derivative of this equation with respect to d_k, considering that the only dependent variable to d_k is R_j^C, results in the following equations:

$$U = \frac{1}{m}\left[\sum_{j=1}^{m}\left(R_j^C - R_j^D\right)^2\right] \quad (8)$$

(7) And (8) → $MF = \sqrt{U}$

$$\rightarrow \frac{\partial \mathrm{MF}}{\partial x} = \frac{1}{2\sqrt{U}}\frac{\partial U}{\partial x} \quad (9)$$

$$(8) \rightarrow \frac{\partial U}{\partial x} = \frac{2}{m}\left[\sum_{j=1}^{m}\left(R_j^C - R_j^D\right)\frac{\partial R_j^C}{\partial x}\right] \quad (10)$$

(9) *and* (10) →

$$\frac{\partial \mathrm{MF}}{\partial x} = \frac{2}{m\mathrm{MF}}\left[\sum_{j=1}^{m}\left(R_j^C - R_j^D\right)\frac{\partial R_j^C}{\partial x}\right]. \quad (11)$$

If we suppose $x = d_k$, then

$$\frac{\partial \mathrm{MF}}{\partial d_k} = \frac{1}{m\mathrm{MF}}\sum_{j=1}^{m}\left[\left(R_j^C - R_j^D\right).\frac{\partial R_j^C}{\partial d_k}\right]. \quad (12)$$

We use (12) to calculate the derivative of the spectrum with respect to d_k[5]:

$$R = \left|r_{L+1,0}\right|^2 = r_{L+1,0}^* r_{L+1,0}. \quad (13)$$

For simplicity, we have neglected the upper and lower indices. Accordingly,

$$r_{k+1,0} = \frac{r_{k+1,k} + r_{k,0}e^{-2j\varphi_k}}{1 + r_{k+1,k}r_{k,0}e^{-2j\varphi_k}} \quad (14)$$

Where *k = 0, 1,...,L,* and $r_{k+1,k}$ equals

$$r_{k+1,k} = \frac{n_{k+1} - n_k}{n_{k+1} + n_k} \quad (15)$$

The optical phase Φ_k is

$$\Phi_k = \frac{2\pi}{\lambda} n_k d_k \quad (16)$$

$r_{k+1,0}$, which is a complex parameter, is

$$r_{k+1,0} = A_{k+1} + jB_{k+1}. \quad (17)$$

According to (13):

$$R = A_{L+1}^2 + B_{L+1}^2. \quad (18)$$

And its derivative with respect to $\mathbf{d_k}$ equals

$$\frac{\partial R}{\partial d_k} = 2\left(A_{k+1}\frac{\partial A_{k+1}}{\partial d_k} + B_{k+1}\frac{\partial B_{k+1}}{\partial d_k}\right) \quad (19)$$

(19) indicates that $\mathbf{A_{k+1}}$ and $\mathbf{B_{k+1}}$ are functions of $\mathbf{d_k}$. Hence, $\frac{\partial A_{k+1}}{\partial d_k}$ may be presented as:

$$\begin{aligned}
\frac{\partial A_{L+1}}{\partial d_k} &= \frac{\partial A_{L+1}}{\partial A_L}\frac{\partial A_L}{\partial d_k} + \frac{\partial A_{L+1}}{\partial B_L}\frac{\partial B_L}{\partial d_k} \\
\frac{\partial A_L}{\partial d_k} &= \frac{\partial A_L}{\partial A_{L-1}}\frac{\partial A_{L-1}}{\partial d_k} + \frac{\partial A_L}{\partial B_{L-1}}\frac{\partial B_{L-1}}{\partial d_k} \\
&\vdots \quad \vdots \quad \vdots \\
\frac{\partial A_{k+2}}{\partial d_k} &= \frac{\partial A_{k+2}}{\partial A_{k+1}}\frac{\partial A_{k+1}}{\partial d_k} + \frac{\partial A_{k+2}}{\partial B_{k+1}}\frac{\partial B_{k+1}}{\partial d_k} \\
\frac{\partial A_{k+1}}{\partial d_k} &= \frac{\partial A_{k+1}}{\partial \Phi_k}\frac{\partial \Phi_k}{\partial d_k} \\
\frac{\partial B_{k+1}}{\partial d_k} &= \frac{\partial B_{k+1}}{\partial \Phi_k}\frac{\partial \Phi_k}{\partial d_k}.
\end{aligned} \quad (20)$$

And $\frac{\partial B_{L+1}}{\partial d_k}$ may also be presented similarly.

5. Fabrication and Measurement

The aforementioned mirror was fabricated using Edwards thermal evaporation device model E306A and Quartz Crystal Thickness Gauge model FTM4 (with the accuracy of (0.5 A°). Pressure of the deposition chamber is 6.10 mbar, and the deposition was carried out on a cold glass substrate. After deposition, the mirror shall be kept away from humidity. By placing a mirror in Elmer Perkin Optical Spectrometer model LAMBDA9 under the angle of zero degree relative to the axis perpendicular to the mirror, the spectrum passed through the mirror, shown in Fig.1, was obtained.

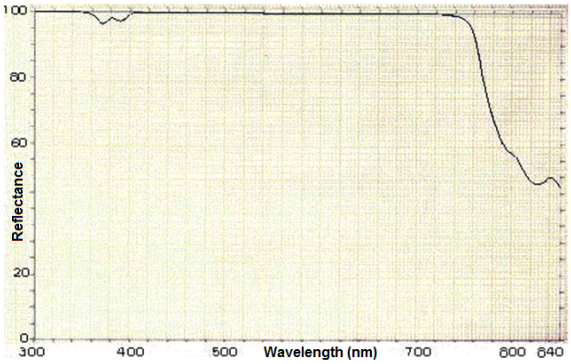

Fig. 1: The Dielectric Mirrors reflectance spectrum.

To improve the coating's durability towards humidity, we can use a layer of cryolite, which has a higher durability, as the final layer. Here, we have used a quarter-wavelength cryolite layer. Furthermore, for a better adhesion between the layers and the substrate, a quarter wavelength of cryolite has been placed on the substrate before starting the deposition. It shall be noted that, according to the evaluations, adding these two layers doesn't have a noticeable impact on the range of the reflectance spectrum and only results in a slight displacement of the reflected beams' phase.

6. Conclusion

The results obtained from the fabrication of this mirror can be summarized into the following points:

- The fabricated mirror has a very high reflection level and a vast reflection area, which is constant all through the substrate. Thus, employing the gradient algorithm has been very useful.
- Using ZnS as a material with a high refraction coefficient exceeds the evaporation process, but the issue of keeping it from humidity is of utmost importance as well. In order to improve the durability of the coating, we can use cryolite as the final layer, which has a higher durability. Stronger materials such as Titanium Dioxide, Zirconium Dioxide or Cranium Dioxide with a refraction coefficient of 2.2 may also be used.

References

[1] Kong, W., et al., Broadband and high efficiency metal–multilayer dielectric grating based on non-quarter wave coatings as reflective mirror for 800 nm. *Journal of Modern Optics*, **59**, 1680–1685 (2012).

[2] Muhammad-Sukki, Firdaus, et al., Mirror symmetrical dielectric totally internally reflecting concentrator for building integrated photovoltaic systems. *Applied energy*., **113**, 32-40 (2014).

[3] Janicki, V., et al., *Multilayer based interferential-plasmonic structure: metal cluster 3D grating combined with dielectric mirror.* Applied physics. A, in Materials science & processing, **103**, 517–519 (2011).

[4] Yun, S., et al., Demonstration of a nearly ideal wavelength-selective optical mirror using a metamaterial-enabled dielectric coating. *Applied Physics Letters*, **102,** 171114 (2013).

[5] Khreis, O. M. Modeling interdiffusion in semiconductor distributed Bragg reflectors: An analytical approach. *Superlattices and Microstructures*., **52**, 913-920 (2012).

[6] Azunre, Paul, et al., Guaranteed global optimization of thin-film optical systems. *New Journal of Physics*., **21**, 1-19 (2019).

[7] Ishimaru, Akira. *Electromagnetic Wave Propagation, Radiation, and Scattering: From Fundamentals to Applications*. John Wiley & Sons, New York: (2017).

[8] Iizuka, Keigo., *Geometrical Optics*, in Engineering Optics, Fourth Edition, Springer International Publishing, Cham, (2019).

[9] Osama M. Khreis, et al., *An error-function compositional grading scheme in vertical-cavity surface-emitting lasers.* 5th International Conference on Electronic Devices, in Systems and Applications (ICEDSA), 1-4 (2016).

[10] Helou, Elias S., et al., Superiorization of preconditioned conjugate gradient algorithms for tomographic image reconstruction. *arXiv preprint arXiv*., **2(2)**, 1-15 (2018).

[11] Rosasco, Lorenzo., et al., Convergence of stochastic proximal gradient algorithm. *Applied Mathematics & Optimization*, 1-27 (2019).